ELEMENTA
Science of the Anthropocene

Ehrlich, J., et al. 2021. Sea-ice associated carbon flux in Arctic spring. *Elem Sci Anth*, 9: 1. DOI: https://doi.org/10.1525/elementa.2020.00169

RESEARCH ARTICLE

Sea-ice associated carbon flux in Arctic spring

J. Ehrlich[1,2,*], B. A. Bluhm[3], I. Peeken[2], P. Massicotte[4], F. L. Schaafsma[5], G. Castellani[2], A. Brandt[6,7], and H. Flores[2]

The Svalbard region faces drastic environmental changes, including sea-ice loss and "Atlantification" of Arctic waters, caused primarily by climate warming. These changes result in shifts in the sea-ice-associated (sympagic) community structure, with consequences for the sympagic food web and carbon cycling. To evaluate the role of sympagic biota as a source, sink, and transmitter of carbon, we sampled pack ice and under-ice water (0–2 m) north of Svalbard in spring 2015 by sea-ice coring and under-ice trawling. We estimated biomass and primary production of ice algae and under-ice phytoplankton as well as biomass, carbon demand, and secondary production of sea-ice meiofauna (>10 μm) and under-ice fauna (>300 μm). Sea-ice meiofauna biomass (0.1–2.8 mg C m^{-2}) was dominated by harpacticoid copepods (92%), nauplii (4%), and Ciliophora (3%). Under-ice fauna biomass (3.2–62.7 mg C m^{-2}) was dominated by *Calanus* copepods (54%). Appendicularia contributed 23% through their high abundance at one station. Herbivorous sympagic fauna dominated the carbon demand across the study area, estimated at 2 mg C m^{-2} day^{-1} for ice algae and 4 mg C m^{-2} day^{-1} for phytoplankton. This demand was covered by the mean primary production of ice algae (11 mg C m^{-2} day^{-1}) and phytoplankton (30 mg C m^{-2} day^{-1}). Hence, potentially 35 mg C m^{-2} day^{-1} of algal material could sink from the sympagic realm to deeper layers. The demand of carnivorous under-ice fauna (0.3 mg C m^{-2} day^{-1}) was barely covered by sympagic secondary production (0.3 mg C m^{-2} day^{-1}). Our study emphasizes the importance of under-ice fauna for the carbon flux from sea ice to pelagic and benthic habitats and provides a baseline for future comparisons in the context of climate change.

Keywords: Arctic Ocean, Biomass, Carbon demand, Primary production, Secondary production, Sympagic fauna

Introduction

The Arctic Ocean harbors a unique ecosystem characterized by organisms that are adapted to an extreme environment comprising polar night, midnight sun, and seasonal or permanent sea-ice cover. The amount of light available for primary production in and under the sea ice is highly variable in space and time and is determined by overall sea-ice cover, sea-ice thickness, snow depth, and sediment in the ice (Gradinger et al., 2009; Massicotte et al., 2019; Castellani et al., 2020). Ice algae tend to be low-light adapted and typically peak in production before the phytoplankton bloom (Leu et al., 2015). Their spring bloom takes place in the bottom centimeters of the sea ice, and they are released to the under-ice environment when the ice is melting later in the season (Gradinger, 2009; Leu et al., 2015). Ice algae can also serve as a food source for under-ice grazers such as ice amphipods or calanoid copepods (Kohlbach et al., 2016). However, the magnitude of ice-algal production tends to be lower than the phytoplankton production, given the much shorter time window for bloom development (Leu et al., 2011). The timing of both blooms is important for the survival and reproduction of ice-associated (sympagic) fauna, which obtains at least part of its food demand from ice algae when phytoplankton is not yet available (Gradinger, 1999a; Søreide et al., 2010; Leu et al., 2011).

The Arctic sea-ice community inside the ice is diverse, comprising bacteria, autotrophic, mixotrophic, and heterotrophic protists (Gradinger, 1999b; Poulin et al., 2011; Hop et al., 2020) and metazoans (Gradinger, 1999a). Although the composition of the heterotrophic sea-ice fauna (sea-ice meiofauna) varies between regions, seasons, and ice types, some taxa widely occur in Arctic sea ice (Bluhm et al., 2018). In terms of abundance, heterotrophic protists are often dominated by Ciliophora, whereas the multicellular fauna is often dominated by herbivorous Harpacticoida and copepod nauplii (Grainger

[1] Centre for Natural History (CeNak), University of Hamburg, Hamburg, Germany
[2] Alfred Wegener Institute, Helmholtz Centre for Polar and Marine Research, Bremerhaven, Germany
[3] Institute of Arctic and Marine Biology, UiT The Arctic University of Norway, Tromsø, Norway
[4] Takuvik Joint International Laboratory, Université Laval, Québec City, Quebec, Canada
[5] Wageningen Marine Research, Den Helder, the Netherlands
[6] Senckenberg Research Institute and Natural History Museum, Frankfurt am Main, Germany
[7] Institute of Ecology, Diversity and Evolution, Goethe University, Frankfurt am Main, Germany

* Corresponding author:
Email: julia.ehrlich@awi.de

and Hsiao, 1990; Gradinger, 1999a; Bluhm et al., 2018; Ehrlich et al., 2020). These and other sea-ice meiofauna taxa are primarily consumers of ice algae and therefore important links in the transfer of energy from the sea ice to pelagic and benthic food webs (Gradinger, 1999a; Nozais et al., 2001; Grebmeier et al., 2010). A recent study by Gradinger and Bluhm (2020) aimed to evaluate the extent of sea-ice meiofauna grazing in landfast ice and the degree to which sea-ice meiofauna, in turn, becomes the prey of larger predators beneath the ice. Their study showed that sea-ice meiofauna has a low grazing impact on the ice-algal spring bloom and leaves the vast majority of organic matter for under-ice, pelagic, and benthic communities.

In addition to biota living inside the sea-ice brine channel system, invertebrates dwelling in the under-ice water layer are important for the carbon transfer to deeper water layers, not the least through their diel and seasonal vertical migration. For example, *Calanus* species have life cycles adapted to food availability during ice-algal and phytoplankton blooms (Søreide et al., 2010). *Calanus glacialis* and *Calanus hyperboreus* comprise the main biomass in the central Arctic Ocean (Auel and Hagen, 2002; Darnis et al., 2008; Kosobokova and Hirche, 2009). They feed on both ice algae and phytoplankton (Kohlbach et al., 2016) and perform seasonal vertical migration to depths of hundreds of meters whereby they contribute significantly to the carbon cycle of the Arctic Ocean (Fortier et al., 2001; Daase et al., 2016; Darnis et al., 2017). Sympagic amphipods, such as *Apherusa glacialis*, also show a high trophic dependency on ice-algal production, emphasizing the role of ice algae for the Arctic marine food web (Werner, 1997; Scott et al., 1999; Kohlbach et al., 2016). In addition, the sympagic realm is inhabited by carnivorous taxa, such as large *Paraeuchaeta* copepods, chaetognaths, the amphipod *Themisto libellula*, and Polar cod *Boreogadus saida*, which are important for providing carbon to the higher trophic levels in ice-covered seas (Welch et al., 1992; Dalpadado, 2002; David et al., 2016).

Earlier studies investigated the community composition and biomass of sea-ice meiofauna (Friedrich, 1997; Gradinger et al., 1999; Gradinger and Bluhm, 2020) and under-ice fauna (Lønne and Gulliksen, 1991; David et al., 2015; Flores et al., 2019) in the Arctic Ocean. Based on comparison with earlier studies, the impact of climate warming on the Arctic sea-ice ecosystem has already altered community compositions. Examples include the virtual absence of Nematoda in pack ice north of Svalbard compared to the 1990s and the changing protist community in the pack ice of the central Arctic Ocean over a 40-year period (Kiko et al., 2017; Ehrlich et al., 2020; Hop et al., 2020). Because sympagic fauna comprises different feeding types accompanied by specific prey preferences, an altered community composition together with an increase of small-sized species in response to global warming will result in a decoupling of predator–prey dynamics, as smaller species favor smaller prey (Daufresne et al., 2009; Li et al., 2009). Earlier studies either assessed the dependency of single species on ice algae and phytoplankton (Werner, 1997; Kohlbach et al., 2016) or estimated the vertical flux from ice floes without the consumer perspective (Moran et al., 2005; Nöthig et al., 2020). However, a holistic compilation of primary production estimates, consumer carbon demands, and secondary productions for the in-ice and the under-ice realm has not been acquired before. Our study aimed at investigating the linkages between sea-ice and under-ice biota and the potential carbon flux from the sympagic realm to the pelagic and benthic systems by:

(1) quantifying the biomass and production rates of ice algae, under-ice phytoplankton, and sympagic fauna in and under Arctic pack ice;
(2) estimating the potential grazing impact of sea-ice meiofauna and under-ice fauna on ice-algal and phytoplankton production, respectively;
(3) evaluating the potential predation impact of carnivorous under-ice fauna on the secondary production; and
(4) assessing the amount of primary production that remains for the pelagic and benthic communities.

Materials and methods

Study area

This study was conducted during the international Transitions in the Arctic Seasonal Sea Ice Zone expedition aboard RV *Polarstern* (PS92) between May 19 and June 28, 2015. All samples were taken in the Eurasian sector of the Arctic Ocean near the Atlantic water inflow north of Svalbard between 7.07–19.91°E and 81.0–82.21°N. We sampled ice cores at 8 ice stations (**Figure 1**). In close vicinity to those ice stations, we also took samples with the Surface and Under-Ice Trawl (SUIT; Flores, 2009; **Figure 1**). Two of the 8 ice stations were located on the marginal shelf north of Svalbard (stations 19 and 32), 4 in the Sophia Basin and on its slope (stations 27, 31, 47, and 39), and 2 at the Yermak Plateau (stations 43 and 45/46; **Figure 1**). During our study, approximately 1.5-year-old sea ice covered on average 65% of the sampling area (Ehrlich et al., 2020). The sampled region is characterized by a strong inflow of Atlantic Water along the West Spitsbergen Current and the Fram Strait branch. This inflow brings the most oceanic heat into the Arctic Ocean and contributes strongly to the observed sea-ice loss in the past decades (Beszczynska-Möller et al., 2012; Rudels et al., 2013). It is also responsible for the advection of zooplankton from sub-Arctic regions (Bluhm et al., 2011).

Processing and parameter estimation of sea-ice biota

Sampling, biomass, and primary production of ice algae at ice stations

A main coring site was established at each ice station, and 4 ice cores were taken to determine different

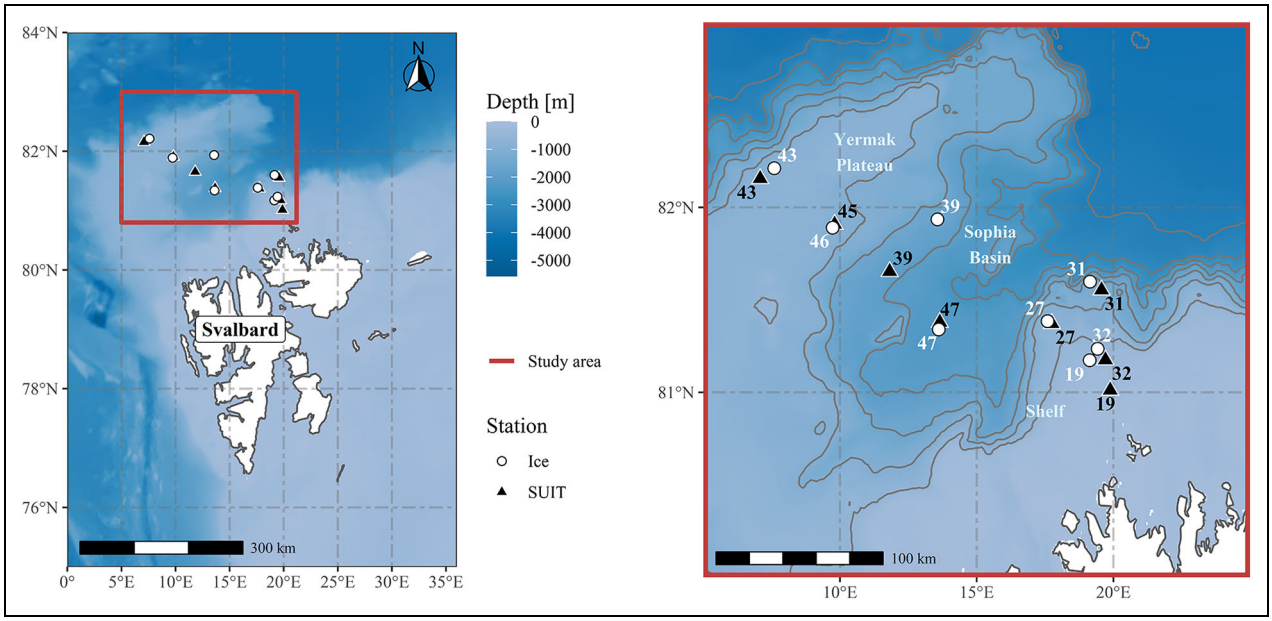

Figure 1. Map of the study area and sampled stations. During the RV *Polarstern* expedition PS92 north of Svalbard, samples were taken at 8 ice stations (white circles) and 8 Surface and Under-Ice Trawl stations (black triangles). DOI: https://doi.org/10.1525/elementa.2020.00169.f1

biogeochemical variables. The ice cores were drilled with a Kovacs corer (Kovacs Enterprise, Roseburg, OR, USA; inner diameter: 9 cm). Two ice cores were taken at each ice station for pigment analysis. The bottom 10 cm of both ice cores were pooled and melted in filtered seawater (0.2 µm). The samples were filtered on GF/F filters and immediately frozen in liquid nitrogen and stored at –80°C until analysis. Chlorophyll *a* (chl *a*) concentrations were measured with high-performance liquid chromatography (HPLC) as described in Tran et al. (2013). The carbon biomass of ice algae for the ice stations was estimated from the sea-ice chl *a* concentrations at each station (Ehrlich et al., 2020), applying an average C:chl ratio of 53 (Vernet et al., 2017), which reflects the overall mixed community of diatoms and flagellates found in our study region (Peeken, 2020).

Photosynthesis–irradiance (PE) curves were measured on a second set of 2 ice cores, which were collected at each ice station. The bottom 1-cm sections of each ice core were transferred in 50 mL of filtered (0.2 µm) surface seawater. Continuous gentle shaking helped to thaw the sample rapidly. All samples were kept in the dark prior to the incubation. PE samples were incubated at different irradiance levels in the presence of ^{14}C-labeled sodium bicarbonate using a method derived from Lewis and Smith (1983). Incubations were carried out in a dimly lit radiation lab under the deck of the vessel to avoid any light stress on the algae. To calculate the primary production using photosynthetic parameters derived from the PE curves, the incoming photosynthetically available radiation at the surface (PAR, E°(PAR, 0+)) was measured at 10-min intervals using a CM 11 global radiation pyranometer (Kipp and Zonen, Delft, the Netherlands) installed in the crow's nest of the RV *Polarstern*. PE parameter means of the 2 replicates derived from each ice station (except for station 19) were used to calculate hourly primary production using the following equation:

$$\mathrm{pp} = \mathrm{ps} \times \left(1 - e^{\left(-\alpha \times \frac{\mathrm{PAR}}{\mathrm{ps}}\right)}\right), \quad (1)$$

where pp is the photosynthetic rate (mgC m^{-3} h^{-1}) at light saturation, α is the photosynthetic efficiency at irradiance close to zero (mgC m^{-3} h^{-1} [µmol photon m^{-2} s^{-1}]$^{-1}$), and ps (mgC m^{-3} h^{-1}) is a hypothetical maximum photosynthetic rate without photoinhibition. Daily primary production rates (µg C m^{-2} day^{-1}) were then calculated by integrating hourly primary production over 24 h (for further details, see Massicotte et al., 2019).

Sampling, biomass, carbon demand, and secondary production of sea-ice meiofauna

Sea-ice meiofauna (here heterotrophs > 10 µm) was sampled at each of the 8 stations. The detailed sampling procedure was as described in Ehrlich et al. (2020). We sampled the lowermost 10 cm of a set of duplicate ice cores per station because the highest sea-ice meiofauna densities are usually found in this bottom layer of the sea ice (Friedrich, 1997; Nozais et al., 2001; Marquardt et al., 2011). Choosing the 10-cm section was a compromise, as that layer accounted for about two-thirds of all sea-ice meiofauna in a pan-Arctic data compilation of over 700 ice cores (Bluhm et al., 2018), while in other studies, all sea-ice meiofauna were found in the bottom 2 cm (Nozais et al., 2001). The faunal concentration in the bottom layer is because this layer has a high probability of colonization by both pelagic and benthic fauna. It is also in free exchange with nutrients from the underlying seawater, which sustain the growth of ice-algal food for many of these taxa (Arndt and Swadling, 2006). A small fraction of sea-ice meiofauna may also be found outside the

sampled bottom ice layer (Bluhm et al., 2018). However, microscopic inspection of the melted top 10-cm section of our ice cores showed an absence of sea-ice meiofauna in this layer. The bottom 10-cm sections were melted separately with the addition of 200 mL of 0.2-µm-filtered seawater per centimeter of ice core to protect the fauna from osmotic stress during melting (Garrison and Buck, 1986). Melting took place onboard in a dark room at 4°C. After melting, the samples were concentrated on 10-µm gauze and fixed in 4% buffered formaldehyde solution until later quantitative analysis. Taxonomic names were verified for correctness and synonymy using the World Register of Marine Species (WoRMS; http://www.marinespecies.org).

The biomass (µg C m^{-2}) for sea-ice meiofauna taxa was calculated by multiplying abundances (ind. m^{-2}) of each taxon obtained from Ehrlich et al. (2020) by the carbon content per individual of this taxon. Carbon content values were taken from the literature (Table S1). To minimize over- and underestimations, we used region-specific data and/or those that covered relevant size spectra whenever possible. If no value for carbon content of a taxon was found, regression equations from the literature were used to calculate the dry weight, and dry weight-to-carbon ratios from literature were used to estimate the carbon content of that particular taxon (Table S1). The mass-specific ingestion rate (% of body C day^{-1}) of each sea-ice meiofauna taxon was calculated according to Gradinger (1999a) with the allometric mass specific equation of Moloney and Field (1989):

$$I_{max} = 63 \times M^{(-0.25)} \times 0.23326, \quad (2)$$

where I_{max} is the daily mass-specific maximum potential ingestion rate (day^{-1}), 63 is the biomass-specific ingestion rate coefficient, M is the biomass of a single organism (pg C), and 0.23326 is the unitless temperature compensation. We assumed a sea-ice temperature of –1°C (for details on physical parameters, see Ehrlich et al., 2020) and a temperature coefficient (Q10) value of 2 (typical for plankton metazoans; Moloney and Field, 1989). The mass-specific ingestion rate of each taxon was then multiplied by the total carbon biomass of that taxon at every station to determine the carbon demand per day (µg C m^{-2} day^{-1}; Table S1). In order to quantify the fraction of ice-algal carbon demand of key herbivorous sea-ice meiofauna taxa (Harpacticoida, nauplii, Ciliophora), we assumed Harpacticoida and nauplii were covering 100% and Ciliophora 50% of their carbon demand by feeding on ice algae (Verity, 1991; Table S1). Although Harpacticoida and nauplii are also known to feed on Ciliophora (Kramer, 2011), the biomass of Ciliophora in comparison to ice algae was so small (<1% of ice-algal biomass) that it was considered negligible. For the calculation of sea-ice meiofauna secondary production, all production-to-biomass (P:B) ratios were obtained from Forest et al. (2014). The P:B ratio of 0.062 for Arctic protozooplankton was used for Ciliophora, Tintinnina, Dinophyceae, and Amoebozoa, and the P:B ratio of 0.021 for Arctic nauplii and small zooplankton was used for Harpacticoida, Nauplii, and Rotifera.

Processing and parameter estimation of under-ice biota

Sampling, biomass, and primary production of ice algae and phytoplankton at SUIT stations

Prior to arriving or directly after leaving each station, a SUIT was deployed. The SUIT consists of a steel frame with a 2 m × 2 m opening, 2 parallel 15-m-long nets, and a sensor package attached to the opening of the SUIT (for sensor details, see Lange et al., 2016). The set of sensors measured environmental variables at each station. Chl *a* concentration of phytoplankton right under the ice was determined by using a fluorometer (Cyclops, Turner Designs, San Jose, CA, USA), which was incorporated in the conductivity, temperature, and depth probe (CTD; Sea and Sun Technology CTD 75M memory probe) and calibrated against chl *a* concentrations measured by HPLC from water column samples. Under-ice irradiance values were measured using Ramses spectral radiometers (Trios GmbH, Rastede, Germany) with a wavelength range from 350 to 920 nm and a resolution of 3.3 nm. From the under-ice hyperspectral measurements, we retrieved ice-algal chl *a* by applying the normalized difference indices algorithm (for details, see Castellani et al., 2020). Due to failure of the sensor package, no data could be collected at stations 31 and 32. In addition, missing hyperspectral measurements at station 27 did not allow for retrieval of ice-algal chl *a* for this station. The measured chl *a* concentrations are available in Ehrlich et al. (2020). The carbon biomass of ice algae and phytoplankton at the SUIT stations was calculated as above for ice algae at ice stations.

Primary production (µg C m^{-2} day^{-1}) for ice algae and phytoplankton at SUIT stations was calculated similarly as for ice algae at ice stations (see previous section). For calculation of the ice-algal primary production, an hourly PAR under the ice was calculated by multiplying E° (PAR, 0+) by the sea-ice transmittance. The sea-ice transmittance was calculated as the ratio between incoming and under-ice light, the latter measured with a RAMSES-ACC irradiance sensor (Trios GmbH, Rastede, Germany) attached to the SUIT. For the calculation of the phytoplankton primary production, we used PE curves determined from additional under-ice water samples, which we collected with Niskin bottles mounted on a Sea-Bird rosette water sampler equipped with a CTD probe (SBE911+) at each ice station. Available light for phytoplankton photosynthesis was estimated by integrating PAR over the first 2 m of the water column under the ice sheet. PAR between 0 and 2 m was propagated into the water column using upward attenuation coefficient calculated from radiance profiles measured from the Remotely Operated Vehicle (for details, see Nicolaus and Katlein, 2013). In the marginal ice zone, large leads often increase the amount of light available to phytoplankton. To account for this additional source of available light, we applied the Method 2 of Massicotte et al. (2019), which aims at averaging production under the ice and in adjacent open waters using a mixing model based on sea-ice concentration derived from satellite imagery to upscale the estimates of primary production derived from the SUIT.

Sampling, biomass, carbon demand, and secondary production of under-ice fauna

Under-ice fauna (here metazoans > 300 μm) was sampled at each of the 8 stations and caught with the 300-μm zooplankton net of the SUIT with a single sample per station. The catch was concentrated on a 100-μm sieve, and a defined fraction was preserved in 4% buffered formaldehyde solution until later quantitative analysis (for details, see Ehrlich et al., 2020). All fauna samples were sorted under stereomicroscopes (Zeiss Discovery.V20 and Leica Model M 205C or a Leica Discovery V8) and identified to the lowest taxonomic level possible. Taxonomic names were verified for correctness and synonymy using the WoRMS (http://www.marinespecies.org).

The biomass (μg C m^{-2}) for all under-ice fauna taxa was calculated by multiplying catch abundances as established in Ehrlich et al. (2020) with the carbon content per individual of the taxon. Carbon (C) values were taken from the literature (Table S2). To minimize over- and underestimations, we used region-specific data and/or those that covered relevant size spectra whenever possible. The mass-specific ingestion rates (% of body C day^{-1}) for the biomass-dominant under-ice taxa (*Calanus* spp., Amphipoda, Chaetognatha, Appendicularia), which combined accounted for 99.5% of the total under-ice fauna biomass, were taken from the literature (Deibel, 1988; Saito and Kiorboe, 2001; Campbell et al., 2016; Table S2). For the remaining taxa, no mass-specific ingestion rates were available; instead, the mean value of the above-mentioned dominant taxa was used (Table S2). The mass-specific ingestion rate of each taxon was then multiplied by the total biomass of that taxon at every station to determine the carbon demand per day (μg C m^{-2} day^{-1}; Table S2). To consider that some of the key herbivores (*C. hyperboreus*, *C. glacialis*, *Calanus finmarchicus*, *A. glacialis*, and Appendicularia) use both ice algae and phytoplankton as food sources in our study area (Kohlbach et al., 2016), we assumed *C. hyperboreus* to cover 25% and *C. glacialis* to cover 33% of their carbon demand from ice algae (Kohlbach et al., 2016). For *C. finmarchicus*, we took the same value as for *C. glacialis* (33%) referring to Søreide et al. (2013), who showed that *C. finmarchicus* feed on a mixture of phytoplankton and ice algae. For *A. glacialis*, we used an ice-algal share of 86% of the total carbon demand (Kohlbach et al., 2016). Because Appendicularia are herbivorous filter feeders, we assumed no prey selectivity and split their carbon demand corresponding to the ratio of ice-algal and phytoplankton primary production at each station. To estimate the total carbon demand of the sea-ice and the under-ice fauna together, we used their means over all 8 stations as representative of the general study area. The secondary production of under-ice fauna was calculated by using a P:B ratio of 0.012 for all taxa obtained from Forest et al. (2014) for large Arctic mesozooplankton species.

Data visualization

All figures were created with R-Software Version 3.6.0 (R Core Team, 2018) and the "ggplot2" package (Wickham, 2016). Additional features of the plots were modified using the packages "scales" (Wickham, 2018) and "ggnewscale" (Campitelli, 2019). The plots were combined in grids using the "ggpubr" package (Kassambara, 2020). Map features were handled with functions from the packages "ggspatial" (Dunnington, 2018) and "sf" (Pebesma, 2018). Bathymetry data were taken from the "marmap" package (Pante and Simon-Bouhet, 2013) and spatial information data of countries from "rnaturalearth" and "rnaturalearthhires" (South, 2017, 2020).

Results

Biomass, carbon demand, and production of the sea-ice biota

The biomass of ice algae in ice cores ranged between 10.5 and 41.9 mg C m^{-2} per station (mean = 22.3 mg C m^{-2}; **Figure 2a**, **Table 1**). Ice-algal primary production ranged from 0.5 to 13.7 mg C m^{-2} day^{-1} (mean = 4.8 mg C m^{-2} day^{-1}; **Figure 2b**, **Table 1**).

The biomass of sea-ice meiofauna ranged between 0.05 and 2.8 mg C m^{-2} per station (mean = 1.1 mg C m^{-2}; **Figure 2a**). Harpacticoida contributed by far the most to the total sea-ice meiofauna biomass (92%; mean = 1.0 mg C m^{-2}; **Figure 3a**, **Table 1**). The remaining biomass was mainly attributed to nauplii (4%) and Ciliophora (3%; **Figure 3a**, **Table 1**). The secondary production of sea-ice meiofauna ranged between 0.002 and 0.06 mg m^{-2} day^{-1} (mean = 0.03 mg C m^{-2} day^{-1}; **Figure 2b**). Most of the secondary production was attributed to Harpacticoida (84%) and Ciliophora (9%; **Table 1**). Estimated carbon demand of the sea-ice meiofauna varied from 0.06 to 1.5 mg C m^{-2} day^{-1} (mean = 0.7 mg C m^{-2} day^{-1}) and followed the same pattern as the biomass, with Harpacticoida (81%), nauplii (9%), and Ciliophora (8%) making up the greatest part of the total sea-ice meiofauna carbon demand (**Figure 2b**, **Table 1**). Altogether their ice-algal demand was estimated at 0.6 mg C m^{-2} day^{-1} (**Table 1**). Except for station 27, the ice-algal demand of these taxa was lower than the ice-algal primary production (**Figure 3b**).

Biomass, carbon demand, and production of the under-ice biota

The biomass of ice algae at SUIT stations ranged between 6.3 and 28.5 mg C m^{-2} (mean = 17.7 mg C m^{-2}; **Figure 4a**). The estimated phytoplankton biomass in the 0–2 m under-ice water ranged between 28.6 and 1,120 mg C m^{-2} across stations (mean = 350 mg C m^{-2}; **Figure 4a**). Ice-algal primary production ranged from 3.7 to 34.5 mg C m^{-2} day^{-1} (mean = 16.9 mg C m^{-2} day^{-1}; **Figure 4b**, **Table 2**). The primary production of phytoplankton ranged between 1.2 and 114 mg C m^{-2} day^{-1} (mean = 30.4 mg C m^{-2} day^{-1}; **Figure 4b**, **Table 2**).

The biomass of under-ice fauna ranged between 3.2 and 62.7 mg C m^{-2} (mean = 22.2 mg C m^{-2}; **Figure 4a**). The majority of the biomass was attributed to the 3 *Calanus* species, which had similar mean biomasses and relative contributions to the under-ice fauna (between 3.1 and 4.5 mg C m^{-2}, and 14% and 20%; **Figure 5a**, **Table 2**). Amphipoda contributed to the total under-ice fauna biomass with a mean of 2.5 mg C m^{-2} and a share of 11%

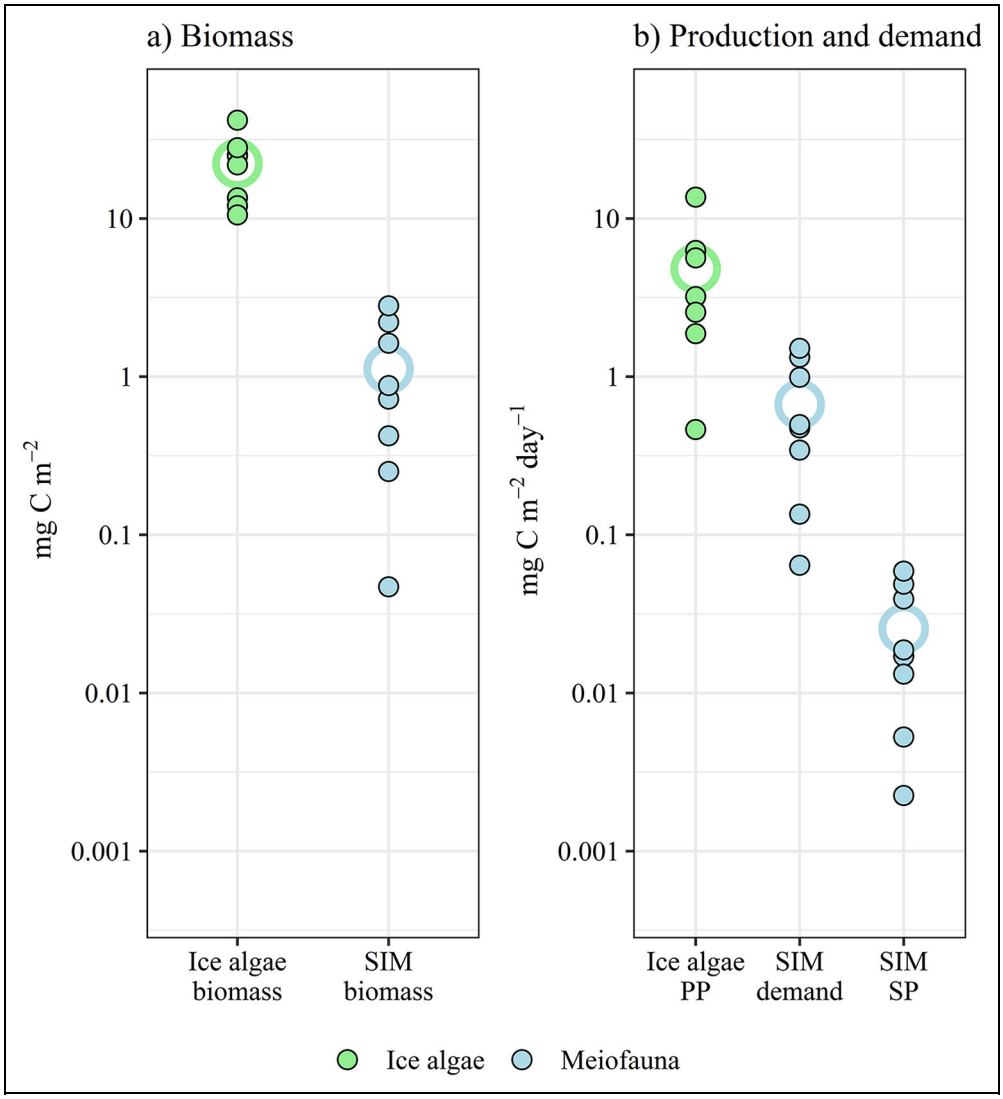

Figure 2. Biomass, carbon demand, and carbon production of ice algae and sea-ice meiofauna. (a) Biomass of ice algae and sea-ice meiofauna (SIM) and (b) ice-algal primary production (PP), SIM carbon demand, and SIM secondary production (SP) across 8 stations north of Svalbard in spring pack ice of 2015. Filled circles represent estimates per station; mean values are marked as unfilled circles. Note that the *y*-axis is $\log_{10}$-scaled. DOI: https://doi.org/10.1525/elementa.2020.00169.f2

(**Table 2**). At station 32, Appendicularia were extremely abundant and made up 23% of the total under-ice fauna biomass (**Figure 5a**, **Table 2**). The combined rest of the under-ice fauna taxa including nauplii, Chaetognatha, and Euphausiacea constituted less than 12% of the biomass (**Table 2**). The secondary production of the under-ice fauna ranged between 0.04 and 0.75 mg C m^{-2} day^{-1} across stations (mean = 0.26 mg C m^{-2} day^{-1}; **Figure 4b**, **Table 2**). Similar to the biomass, most of the secondary production was attributed to the 3 *Calanus* species with means ranging between 0.04 and 0.05 mg C m^{-2} day^{-1}, making up 53% of the secondary production (**Table 2**). Appendicularia had a mean share of 23% and Amphipoda of 11% to the total secondary production (**Table 2**). The carbon demand of the under-ice fauna varied from 0.2 to 29.4 mg C m^{-2} day^{-1} across stations (mean = 5.6 mg C m^{-2} day^{-1}; **Figure 4b**, **Table 2**). Taxa that made up most of the total carbon demand of the under-ice fauna were Appendicularia (59%), *C. finmarchicus* (13%), *C. hyperboreus* (10%), *C. glacialis* (8%), and Amphipoda (1%; **Table 2**). Jointly, their estimated mean carbon demand was 1.3 mg C m^{-2} day^{-1} for ice algae and 3.8 mg C m^{-2} day^{-1} for phytoplankton (**Table 2**). Their ice-algal carbon demand was always lower than the ice-algal primary production at SUIT stations (**Figure 5**), which was not the case for the phytoplankton carbon demand of the under-ice fauna; at station 45, that demand exceeded phytoplankton production by a factor of 1.9 (**Figure 5b**). The mass appearance of Appendicularia at station 32 resulted in a local peak (26.4 mg C m^{-2} day^{-1}) of the herbivorous carbon demand.

Total biomass, carbon demand, and production of sympagic biota

Mean algal biomass (phytoplankton and ice algae combined) was estimated at 372 mg C m^{-2} with a primary

Table 1. Mean biomass, primary production, secondary production, and carbon demand for sea-ice biota at the 8 ice stations, including standard deviation (*SD*, $n = 8$), range, and relative (Rel.) share. DOI: https://doi.org/10.1525/elementa.2020.00169.t1

	Biomass				Primary or Secondary Production				Carbon Demand			
Sea-Ice Biota	Mean (μg C m^{-2})	*SD*	Range	Rel. (%)	Mean (μg C m^{-2} day^{-1})	*SD*	Range	Rel. (%)	Mean (μg C m^{-2} day^{-1})	*SD*	Range	Rel. (%)
Primary producers												
Ice algae	22,300	10,400	10,500–41,900	na[a]	4,810	4,400	463–13,700	na	na	na	na	na
Secondary producers (sea-ice meiofauna)												
Harpacticoida G.O. Sars, 1903	1,030	970	0–2,770	91.6	21.6	20.4	0–58.1	84.7	542 (542)[b]	512	0–1,460	81.1
Nauplii (Copepoda Milne Edwards, 1840)	48.6	46.7	3.3–154	4.3	1.0	1.0	0.1–3.2	4.0	60.0 (60.0)[b]	57.7	4.1–190	9.0
Rotifera Cuvier, 1817	2.4	5.0	0–13.6	0.2	0.2	0.3	0–0.9	0.6	2.9	5.9	0–16.3	0.4
Ciliophora, not documented	37.0	37.6	0–94.2	3.3	2.3	2.3	0–5.8	9.0	53.1 (26.6)[b]	53.9	0–135	7.9
Tintinnina Kofoid and Campbell, 1929	5.3	6.3	0–16.8	0.5	0.3	0.4	0–1.0	1.3	7.6	9.1	0–24.1	1.1
Dinophyceae Fritsch, 1927	1.3	2.1	0–4.9	0.1	0.1	0.1	0–0.3	0.3	2.2	3.6	0–8.5	0.3
Amoebozoa Lühe, 1913, emend. Cavalier-Smith, 1998	0.1	0.3	0–0.9	<0.1	<0.1	<0.1	0–0.1	<0.1	0.2	0.5	0–1.3	<0.1
Total	1,120	993	47–2,810	100	25	21	2–59	100	668 (628)[b]	543	64–1,510	100

[a]Not applicable.

[b]Of that ice algae.

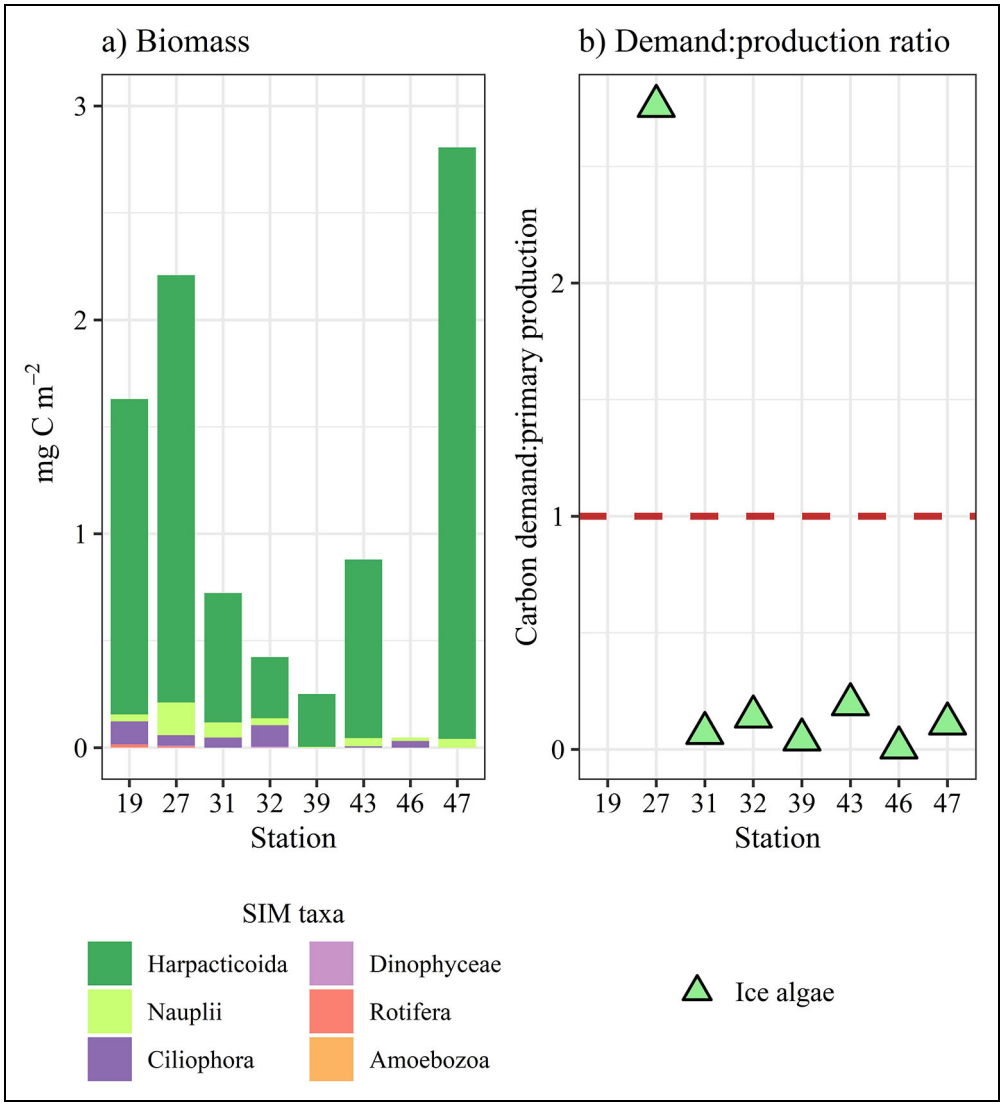

Figure 3. Biomass of sea-ice meiofauna (SIM) taxa and demand: Production ratios at each ice station. (a) Biomass of SIM taxa per station and (b) ratio of carbon demand of herbivorous SIM (Harpacticoida, nauplii, and Ciliophora combined) versus ice-algal primary production per station. In (b), the primary production for station 19 could not be calculated because no photosynthesis–irradiance curve was established for this station. DOI: https://doi.org/10.1525/elementa.2020.00169.f3

production of 41 mg C m^{-2} day^{-1}. Ice algae accounted for 27% of this production (**Table 3**). Mean biomass of the sympagic fauna (sea-ice meiofauna and under-ice fauna combined) was estimated at 23 mg C m^{-2}, of which sea-ice meiofauna accounted for 5%. The carbon demand of the sympagic fauna was estimated at a mean of 6 mg C m^{-2} day^{-1}, of which sea-ice meiofauna accounted for 12% (**Table 3**). The mean secondary production of all sympagic taxa combined was 0.3 mg C m^{-2} day^{-1}, of which sea-ice meiofauna produced 9% (**Table 3**).

Discussion

Primary production of sympagic algae

Since the late 1990s, phytoplankton primary production over the entire Arctic Ocean has increased by approximately 30%, mainly due to a decrease in sea-ice extent and thickness and an increased nutrient supply (Arrigo and van Dijken, 2015; Ardyna and Arrigo, 2020). In general, annual phytoplankton production tends to exceed ice-algal production in the Arctic Ocean basins and on the shelves (Wiedmann et al., 2020). To what degree ice algae contribute to primary production depends on the season, region, and prevailing ice type (Gosselin et al., 1997; Fernández-Méndez et al., 2015). In an earlier study from the central Arctic Ocean, ice algae contributed up to 57% to the primary production in summer (Gosselin et al., 1997). In contrast, in a more recent study conducted during the historical sea-ice minimum in summer 2012, ice algae contributed only up to 30% to total primary production in first-year sea ice (Fernández-Méndez et al., 2015). In our spring study (with approximately 1.5-year-old pack ice and a mean ice coverage of 65%; Ehrlich et al., 2020), 27% of the total sympagic primary production was attributed to ice algae. Our estimated ice-algal production rate (11 mg C m^{-2} day^{-1}) and under-ice phytoplankton production rate (30 mg C m^{-2} day^{-1}) were also well within

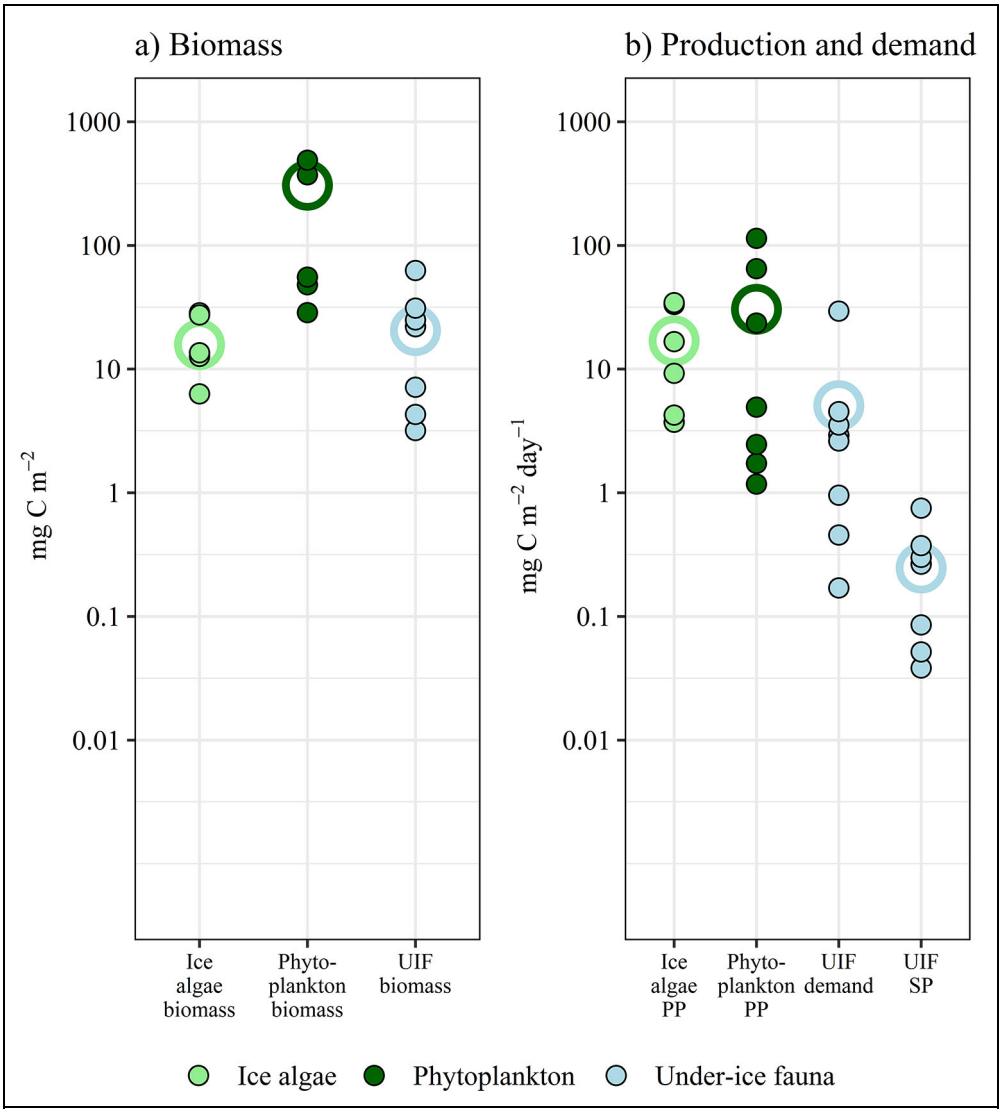

Figure 4. Biomass, carbon demand, and carbon production of ice algae, phytoplankton, and under-ice fauna (UIF). (a) Ice algae, phytoplankton (0–2 m depth), and UIF biomass and (b) ice algae and phytoplankton primary production, and UIF carbon demand and secondary production across 8 stations north of Svalbard in spring pack ice of 2015. Filled circles represent estimates per station; mean values are marked as unfilled circles. Note that the *y*-axis is $\log_{10}$-scaled. DOI: https://doi.org/10.1525/elementa.2020.00169.f4

the range of estimates from the previous summer study of Fernández-Méndez et al. (2015; ice algae 1–13 mg C m^{-2} day^{-1}, phytoplankton: 0.1–60 mg C m^{-2} day^{-1}). These findings indicate that carbon contributions from the sea ice might be more important than some previous studies had assumed (Dupont, 2012; Matrai et al., 2013; Assmy et al., 2017). This result is even more important when considering future model projections, which indicate further increase of ice-algal production in those areas where sea ice persists (Tedesco et al., 2019).

Estimates of primary production by ice algae, however, should be viewed with caution, as their patchy distribution might bias estimations and they show rather a snapshot in time and space (Lange et al., 2017). Some underestimation of the ice-algal primary production may have occurred in our measurements from the lowermost 10 cm of the sampled ice cores because ice algae in certain ice types may be present throughout the ice core (Horner et al., 1992). In our study, ice algae were sampled from first-year sea ice in spring, which in the Arctic typically shows no significant biomass above 10 cm from the sea-ice bottom. The effect of such a potential underestimation therefore would be minimal and not change the main conclusion of this study. Our spatially integrated SUIT-based estimates were about 4 times higher than local ice core–based measurements, confirming that large-scale variability of ice-algal primary production can significantly exceed the variability covered by local measurements (Lange et al., 2017). In our study, we could not separate effects of the sampling scale from those attributed to the different ways used to estimate primary production. However, our findings will be useful for the calibration and validation of biogeochemical models (Tedesco et al., 2019) that upscale the results to the pan Arctic and for comparison with satellite measurements (Ardyna et al., 2014).

Table 2. Mean biomass, primary production, secondary production, and carbon demand for under-ice biota at the 8 ice stations, including standard deviation (*SD*, $n = 8$), range, and relative (Rel.) share. DOI: https://doi.org/10.1525/elementa.2020.00169.t2

	Biomass				Primary or Secondary Production				Carbon Demand			
Under-Ice Biota	Mean (μg C m^{-2})	*SD*	Range	Rel. (%)	Mean (μg C m^{-2} day^{-1})	*SD*	Range	Rel. (%)	Mean (μg C m^{-2} day^{-1})	*SD*	Range	Rel. (%)
Primary producers												
Phytoplankton (0–2 m)	352,000	423,000	28,600–1,120,000	na[a]	30,400	43,500	1,180–114,000	na	na	na	na	na
Ice algae	17,700	9,790	6,300–28,500	na	16,900	13,900	3,720–34,500	na	na	na	na	na
Secondary producers (under-ice fauna)												
Tisbe Lilljeborg, 1853 spp.	<0.1	<0.1	0–0.1	<0.1	<0.1	<0.1	0–0.0	<0.1	<0.1	<0.1	0–0.0	<0.1
Oithona Baird, 1843 sp.	<0.1	<0.1	0–0.0	<0.1	<0.1	<0.1	0–0.0	<0.1	0.0	0.0	0–0.0	<0.1
Calanus hyperboreus Krøyer, 1838	4,390	5,070	5.1–15,800	19.8	52.6	60.8	0.1–189	19.8	560 (140)[b]	634	1.3–1,990	10.0
Calanus glacialis Jaschnov, 1955	3,120	2,210	127–5,960	14.0	37.4	26.5	1.5–71.5	14.0	448 (148)[b]	299	15.7–758	8.0
Calanus finmarchicus (Gunnerus, 1765)	4,540	3,770	492–12,420	20.5	54.5	45.2	5.9–149	20.5	734 (242)[b]	728	59.9–2,380	13.2
Nauplii (Copepoda)	575	1,510	0–4,310	2.6	6.9	18.1	0–51.8	2.6	144	378	0–1,080	2.6
Paraeuchaeta Scott, 1909 spp.	5.6	15.7	0–44.5	<0.1	0.1	0.2	0–0.5	<0.1	1.1	3.1	0–8.9	<0.1
Metridia longa (Lubbock, 1854)	15.9	44.9	0–127	0.1	0.2	0.5	0–1.5	0.1	3.2	9.0	0–25.4	0.1
Clausocalanidae Giesbrecht, 1893	8.7	18.1	0–52.8	<0.1	0.1	0.2	0–0.6	0.0	1.7	3.6	0–10.6	<0.1
Themisto Guerin, 1825 spp.	39.2	110.9	0–313.6	0.2	0.5	1.3	0–3.8	0.2	1.0	2.8	0–7.8	<0.1
Themisto libellula (Lichtenstein in Mandt, 1822)	2.6	4.0	0–10.8	<0.1	<0.1	<0.1	0–0.1	<0.1	0.1	0.1	0–0.3	<0.1
Apherusa glacialis (Hansen, 1888)	2,480	2,460	77.4–6,580	11.2	29.7	29.5	0.9–78.9	11.2	62.0 (53.3)[b]	61.5	1.9–164	1.1
Onisimus glacialis (G. O. Sars, 1900)	2.9	8.2	0–23.3	<0.1	<0.1	0.1	0–0.3	<0.1	0.1	0.2	0–0.6	<0.1
Thysanoessa longicaudata Krøyer, 1846	38.6	94.1	0–270	0.2	0.5	1.1	0–3.2	0.2	7.7	18.8	0–53.8	0.1
Isopoda Latreille, 1817	1.6	4.1	0–11.6	<0.1	<0.1	<0.1	0–0.1	0.0	0.3	0.8	0–2.3	<0.1
Zoaea larvae	<0.1	0.1	0–0.4	<0.1	<0.1	<0.1	0–0.0	<0.1	<0.1	<0.1	0–0.1	<0.1
Cirripedia Burmeister, 1834	17.4	20.2	0.1–59.6	0.1	0.2	0.2	0–0.7	0.1	3.5	4.0	0–11.9	0.1
Chaetognatha not documented	459	1,300	0–3,670	2.1	5.5	15.6	0–44.1	2.1	78.1	221	0–625	1.4
Eukrohnia hamata (Moebius, 1875)	1,270	1,490	0–3,640	5.7	15.3	17.8	0–43.6	5.7	217	253	0–618	3.9

Parasagitta elegans (Verrill,1873)	64.8	107	0–319	0.3	0.8	1.3	0–3.8	0.3	11.0	18.2	0–54.3	0.2
Appendicularia Fol, 1874	5,150	14,600	0–41,200	23.2	61.8	175	0–494	23.2	3,300 (725)[b]	9,320	0–26,400	59.2
Osteichthyes larvae	0.4	1.2	0–3.3	<0.1	<0.1	<0.1	0–0.0	<0.1	0.1	0.2	0–0.7	<0.1
Limacina helicina (Phipps, 1774)	0.1	0.2	0–0.6	<0.1	<0.1	<0.1	0–0.0	<0.1	<0.1	<0.1	0–0.1	<0.1
Clione limacina (Phipps, 1774)	10.9	30.9	0–87.3	<0.1	0.1	0.4	0–1.1	0.0	2.2	6.2	0–17.4	<0.1
Polychaeta Grube, 1850	<0.1	<0.1	0–0.0	<0.1	<0.1	<0.1	0–0.0	<0.1	<0.1	<0.1	0–0.0	<0.1
Trochophora larvae	3.11	7.41	0–21.3	<0.1	<0.1	0.1	0–0.3	<0.1	0.6	1.5	0–4.3	<0.1
Hydrozoa Owen, 1843	<0.1	<0.1	0–0.0	<0.1	<0.1	<0.1	0–0.0	<0.1	<0.1	<0.1	0–0.0	<0.1
Xenacoelomorpha Philippe, Brinkmann, Copley, Moroz, Nakano, Poustka, Wallberg, Peterson & Telford, 2011	0.36	0.64	0–1.7	<0.1	<0.1	<0.1	0–0.0	<0.1	0.1	0.1	0–0.3	<0.1
Total	*22,200*	*19,400*	*3,180–62,700*	*100*	*266*	*233*	*38–752*	*100*	*5,570 (1,310)*[b]	*9,750*	*170–29,400*	*100*

[a]Not applicable.

[b]Of that ice algae.

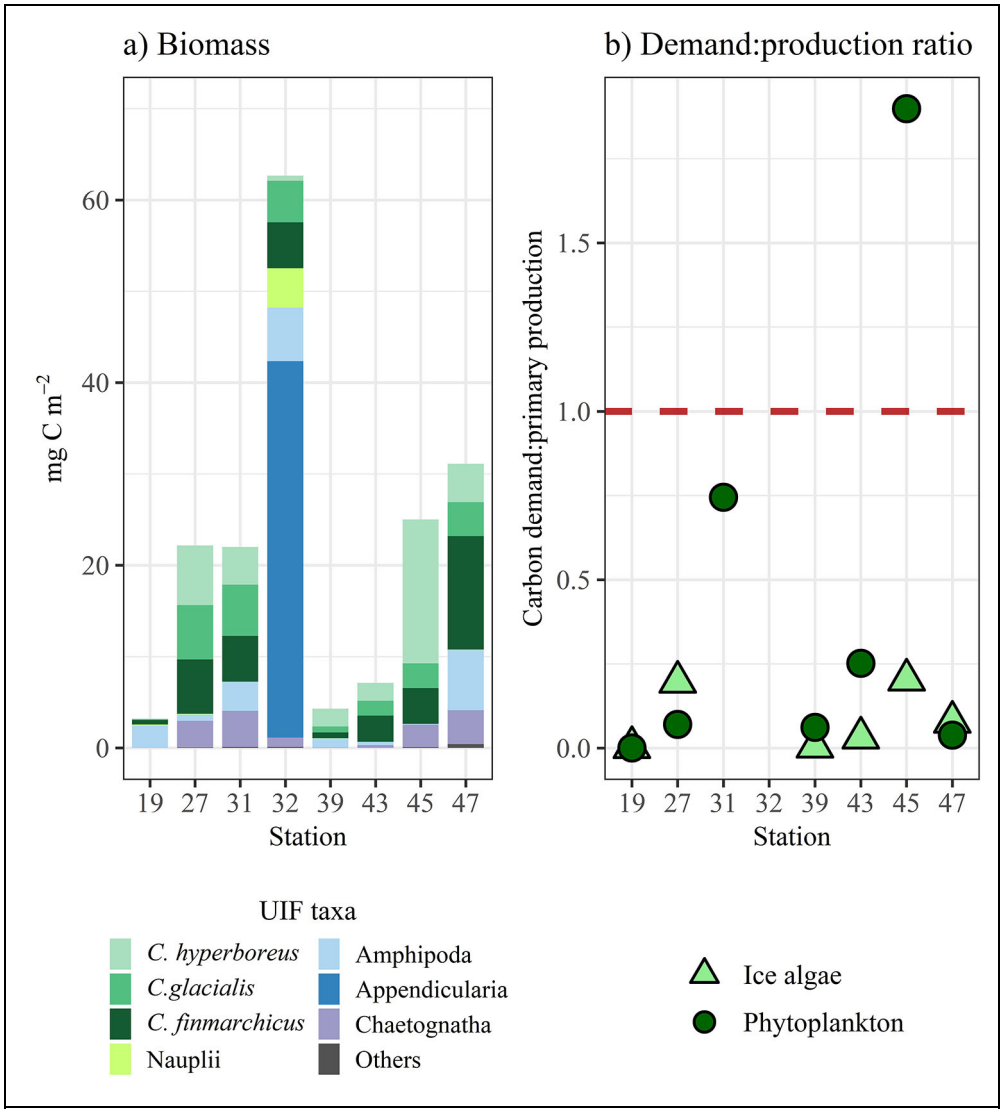

Figure 5. Biomass of under-ice fauna (UIF) taxa and demand: Production ratios at each SUIT station. (a) Biomass of UIF taxa per station and (b) ratio of carbon demand of herbivorous UIF versus ice-algal primary production (PP) and versus phytoplankton PP per station. Ice-algal PP estimates were not available for stations 31 and 32; phytoplankton PP estimates were not available for station 32. DOI: https://doi.org/10.1525/elementa.2020.00169.f5

Table 3. Total biomass, production, and carbon demand of sympagic biota. DOI: https://doi.org/10.1525/elementa.2020.00169.t3

Community	Parameter	Concentration (mg C m^{-2})	Rate (mg C m^{-2} day^{-1})	In-Ice (%)	Under-Ice (%)
Primary producers	Total biomass	372	na[a]	6	94
	Total primary production	na	41	27	73
Secondary producers	Total biomass	23	na	5	95
	Total carbon demand	na	6	12	88
	Total secondary production	na	0.3	9	91

[a]Not applicable.

Biomass, carbon demand, and secondary production of sympagic fauna

The estimated mean biomass of sea-ice meiofauna in our study area (1 mg C m^{-2}) is within the range of earlier estimations from the central Arctic Ocean of <0.1–7.4 mg C m^{-2} (Gradinger, 1999a). However, in Gradinger (1999a), Acoela (then called Turbellaria; 27%), Crustacea (22%), Nematoda (20%), and Ciliophora (15%) dominated the biomass, whereas in our study, Harpacticoida (92%) was the most dominant taxon, followed by copepod nauplii (4%) and Ciliophora (3%). Nematoda and Acoela were neither present in the pack ice of our study nor during the 6-month long Norwegian young sea ice cruise (N-ICE2015) in the same year (Bluhm et al., 2018; Granskog et al., 2018). This absence is assumed to be a consequence of the ongoing change from a multiyear to an annual sea-ice system in this part of the Arctic Ocean (Kiko et al., 2017) and is discussed in more detail in Ehrlich et al. (2020). The transition to a taxon-depleted system may have happened in the early 2000s when Kramer (2011) found Ciliophora and Harpacticoida dominating the biomass of the sea-ice meiofauna, but also still found some Acoela and Nematoda in the ice of the central Arctic Ocean in summer.

The mean carbon demand of the sea-ice meiofauna in our study (0.7 mg C m^{-2} day^{-1}) was also within the range of earlier estimates from Gradinger (1999a; <0.1–7.9 mg C m^{-2} day^{-1}), though in Gradinger (1999a) protists (36%) made up the main grazing impact, whereas Harpacticoida (81%) were the main grazers in our study. This difference indicates that strong taxonomic composition changes do not necessarily affect the overall grazing pressure of sea-ice meiofauna. In the Arctic spring season, increasing daylight allows the development of a strong ice-algal bloom (Leu et al., 2015; Castellani et al., 2017), enhancing the food availability for herbivorous sea-ice meiofauna, such as Harpacticoida. Ice algae usually thrive at the bottom of the ice cover where nutrients in the underlying water are accessible. In contrast, sea-ice meiofauna of higher mobility can actively move in the brine channels, which are usually widest in the lowermost 10 cm of an ice core during the spring season. The ability of sea-ice meiofauna to take advantage of the rich ice-algal food source is therefore assumed. Earlier studies (excluding Ciliophora) suggested a negligible grazing impact of sea-ice meiofauna on the spring bloom (Nozais et al., 2001; Gradinger, 2009; Gradinger and Bluhm, 2020). While we did include Ciliophora grazing, which accounted for 8% of the mean sea-ice meiofauna carbon demand, sea-ice meiofauna still grazed only 14% of the mean ice-algal primary production. Again, our estimate may be conservative, given that the possible presence of sea-ice meiofauna higher up in the core was not considered. We had a single station where the estimated carbon demand of sea-ice meiofauna was 2.8 times higher than the ice-algal primary production (station 27). This discrepancy suggests that on a local scale, sea-ice meiofauna might have a decisive grazing impact on ice algae, which then in turn would not provide sufficient carbon for the local under-ice communities.

A recent study, using the same method to sample under-ice fauna as ours, reported a mean under-ice fauna biomass of 7 mg C m^{-2} in the central Arctic Ocean in autumn, dominated by the ice-associated amphipod *A. glacialis* and the copepod species *C. glacialis* and *C. hyperboreus* (Flores et al., 2019). In our spring study, the mean under-ice fauna biomass was 3-fold higher (22 mg C m^{-2}) and dominated by the 3 *Calanus* species (*C. hyperboreus*, *C. glacialis*, and *C. finmarchicus*). The extremely high abundance of Appendicularia at one station elevated the biomass in our study by 5 mg C m^{-2}. *Calanus* species are well known to be among the main contributors to the biomass of under-ice fauna in the Arctic Ocean (Werner, 2006). However, Appendicularia have not been reported in such high biomass directly under the sea ice in this area, though they were observed frequently in surface waters of the ice-covered Canada Basin (Raskoff et al., 2010) and locally in the Nansen Basin (David et al., 2015). In contrast to other studies from the Arctic Ocean (Werner, 2006; Flores et al., 2019), the ice amphipod *A. glacialis* did not dominate the sympagic biomass in this study. *A. glacialis* represents an important food source for other ice-associated fauna such as polar cod, seabirds, and seals (Bradstreet and Cross, 1982; Werner, 1997; Kohlbach et al., 2017) and is therefore considered as an important link for carbon transfer from lower to higher trophic levels in the Arctic marine food web. The low biomass of ice amphipods in our study is consistent with the observed decline of sympagic amphipod biomass in the European Arctic sector over the past decades (CAFF, 2017). The low abundances of *A. glacialis* may be related to a recent interruption of the Transpolar Drift (Krumpen et al., 2019). Assuming that *A. glacialis* colonizes the sea ice in waters off Siberia to drift across the central Arctic Ocean before potentially returning to the source area with deep currents (Berge et al., 2012), the increasing decay of sea ice along the Transpolar Drift may have released ice amphipods in the central Arctic basins. Thus, only low abundances were left to recolonize the newly formed ice during its drift toward our study area.

Most of the total carbon demand of the under-ice fauna (6 mg C m^{-2} day^{-1}) was attributed to Appendicularia (at a single location), and the copepods *C. finmarchicus*, *C. hyperboreus*, and *C. glacialis*, all of which are considered to be mainly herbivorous feeders (Stevens et al., 2004). Previous studies focused in particular on the grazing impact of sympagic amphipods on ice algae (Werner and Auel, 2005; Hop and Pavlova, 2008; Kohlbach et al., 2016). However, our study estimated that the 3 *Calanus* species together had up to a 9 times higher ice-algal carbon demand than the amphipod *A. glacialis*. In addition, the patch of high Appendicularia biomass resulted in an estimated grazing impact similar to that of all *Calanus* spp. together. These results show how patchiness can result in a local boost of carbon demand and therefore lower algal carbon export to other trophic levels. The results also show that all dominant taxa need to be considered when determining the grazing pressure on ice algae and estimating carbon fluxes in a holistic assessment. By comparison, the mean carbon demand of the under-ice fauna in our study was one order of magnitude higher than that estimated

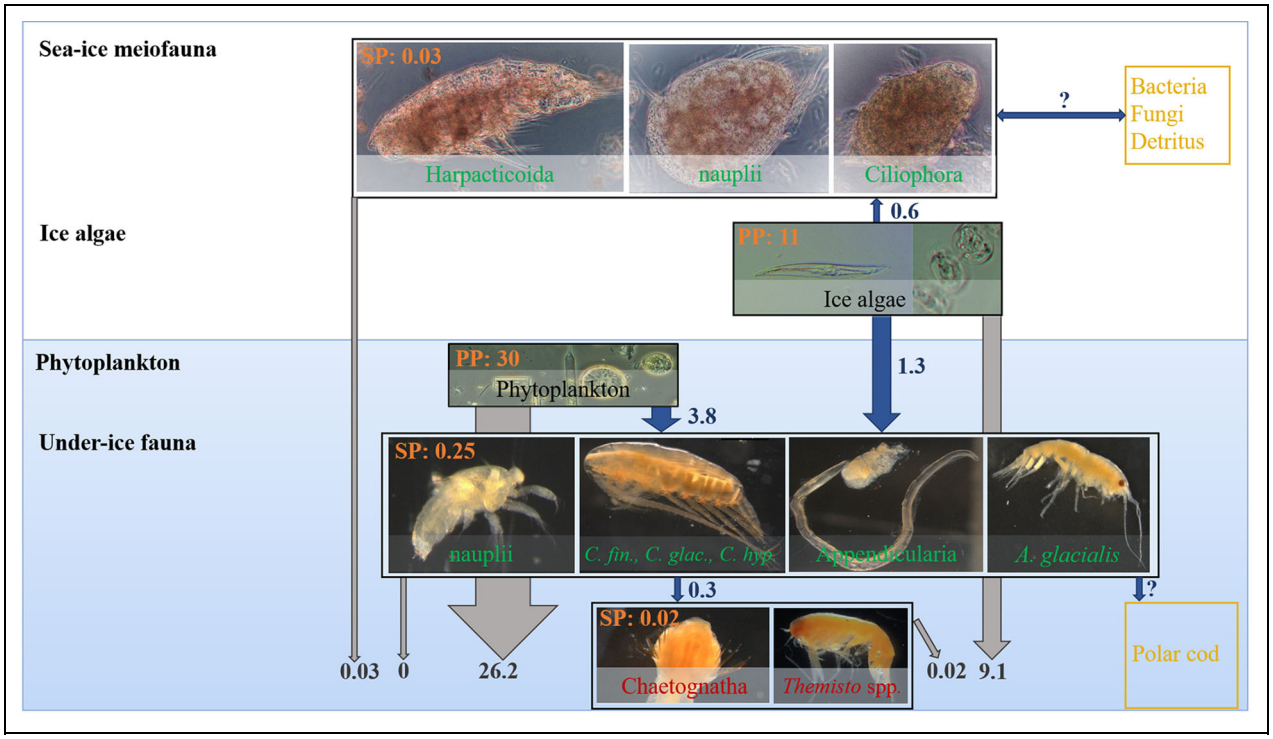

Figure 6. Carbon flux of sympagic biota. Estimated trophic relationships regarding carbon production, consumption, and carbon export (all values are means in mg C m^{-2} day^{-1}) for the sympagic biota of the Atlantic inflow area north of Svalbard in spring. Font colors: Green indicates key taxa of this study that are considered to be mainly herbivorous (including *Calanus finmarchicus*, *Calanus glacialis*, *Calanus hyperboreus*, and *Apherusa glacialis*); red: key taxa of this study considered to be carnivorous; yellow: other taxa (including detritus as a potential carbon source) not included in this study; orange: mean production rate for the respective compartment of the sympagic biota; blue: mean ingestion of the respective consumer; and gray: estimated carbon surplus from the respective sympagic compartment, which is potentially released to the water column. Arrows point in the direction of possible carbon flux; thickness of arrows corresponds to the amount of carbon flux. PP = primary production; SP = secondary production. Photographs by Julia Ehrlich. DOI: https://doi.org/10.1525/elementa.2020.00169.f6

for the central Arctic Ocean in autumn (0.3 mg C m^{-2} day^{-1}; Flores et al., 2019).

As a key feeder on ice algae, *C. glacialis* has timed its seasonal migration and reproduction to the ice-algal bloom (Søreide et al., 2010; Leu et al., 2011). Thus, ongoing sea-ice melt may cause a mismatch between the bloom and developmental stages of *C. glacialis* or may cause decreasing ice-algal production on the long term as ice cover declines. Both aspects are considered to entail negative consequences for the entire Arctic marine food web. However, some studies predict a replacement of *C. glacialis* by the smaller (and less energy-rich) *C. finmarchicus* with increasing "Atlantification" of the Arctic Ocean (Bonnet et al., 2005; Richardson, 2008; Polyakov et al., 2017). The higher biomass of *C. finmarchicus* compared to *C. glacialis* in this study could indicate the hypothesized replacement. As for biomass and carbon demand, the estimated secondary production of the under-ice fauna was also one order of magnitude higher in our study (0.3 mg C m^{-2} day^{-1}) compared to the study of Flores et al. (2019) in the central Arctic Ocean in autumn (0.1 mg C m^{-2} day^{-1}). The seasonal population growth of copepods in our study compared to postbloom collapse and beginning seasonal migration at the end of summer (David et al., 2015) is probably a major reason for this difference.

Cryopelagic coupling

Our study is the first with a comprehensive approach to determine the trophic dependencies between the sympagic fauna and flora assemblages of the Arctic pack-ice in spring (**Figure 6**). By identifying the dominating biomass and demand of herbivorous key taxa, we aimed to disentangle the roles of ice algae and phytoplankton in our study area (**Figure 6**). Our results show that the potential demand for ice-algal carbon was one-third of that for phytoplankton, which highlights the current importance of ice algae for the survival of sympagic communities. In general, growth and successful reproduction of higher trophic levels are equally dependent on the quantity and quality of algae. Ice algae are known not only to constitute a high quality food source (Leu et al., 2011; Kohlbach et al., 2016) but also to provide *Calanus* spp. and other key taxa of the sympagic realm with carbon weeks before the phytoplankton bloom develops and, thus, to ensure successful reproduction (Søreide et al., 2010).

Our study shows that sympagic herbivores do not have the potential to control ice-algal production or phytoplankton production in the Arctic spring (**Figure 6**). Thus, a surplus of approximately 9.1 mg C m^{-2} day^{-1} of ice-algal carbon and 26.2 mg C m^{-2} day^{-1} of (under-ice) phytoplankton carbon could potentially sink to the pelagic and

benthic habitats to provide carbon for the deeper living communities. The pelagic grazers sampled in the under-ice habitat (especially *Calanus* spp.), however, constituted only a fraction of their total population in the upper 100 m, which is in constant exchange with the under-ice environment. This exchange implies that a large proportion of the remaining algal production is probably consumed in the epipelagic layer, before sinking into even deeper layers.

A different pattern was apparent for the carnivorous sympagic fauna in that estimated carbon demand was barely covered by sympagic secondary production. This finding could indicate that the sea-ice habitat is characterized by high competition for prey and that predators may control secondary production in the under-ice water layer. Under-ice predators possibly also fed on microzooplankton (Verity et al., 2002), which was not efficiently caught with the 300-µm net of the SUIT and is therefore underestimated in our secondary production calculations. Furthermore, we assume that most carnivores (Chaetognatha, *Themisto* spp.) are vertically mobile and cover a part of their carbon demand from deeper-dwelling prey. Polar cod (*B. saida*) is an important predator (David et al., 2016) that is not considered in this study. Young polar cod inhabit the under-ice water layer and feed on *A. glacialis*, *Calanus* spp., and the harpacticoid *Tisbe* spp. (Kohlbach et al., 2017). During the sampling for the present study, polar cod were caught in low numbers with the larger 7-mm (half-mesh) SUIT net (data not shown) but appear to be underestimated in the catches (David et al., 2016). Therefore, an unknown but likely significant additional carbon demand of this species would need to be added to the carbon budget.

Conclusions

Putting together a carbon budget that compiles the biomass, carbon demand, and production of sympagic biota shows that our estimates essentially match the 10% law of transfer of energy from one trophic level to another (Lindeman, 1942). The amount of sympagic primary production in Arctic spring was more than sufficient to cover the carbon demand of the herbivorous sympagic fauna both in and under Arctic pack ice. Under-ice fauna was the main contributor to the cryo-pelagic carbon flux, whereas the contribution of sea-ice meiofauna was low. The 3 *Calanus* species (*C. finmarchicus*, *C. glacialis*, and *C. hyperboreus*) dominated the grazing impact under the ice both on ice algae and phytoplankton. Our quantitative assessment supports the notion that the 3 *Calanus* species are key drivers of the Arctic marine ecosystem, transferring energy-rich lipid compounds and essential fatty acids to higher trophic levels. As these species rely on ice algae as food source besides phytoplankton (Kohlbach et al., 2016), the predicted sea-ice loss and with it the decrease of ice algae will lead to a shift in carbon sources for these herbivorous taxa. Phytoplankton production may help to offset potential decreases of ice-algal production to a certain extent. However, a restriction of the ice-algal bloom would also increase the probability of a mismatch between food availability and ontogenetic development, particularly for *C. glacialis*. The secondary production of the sympagic fauna was barely sufficient to support the carbon demand of carnivorous under-ice taxa. Subsequently, predators might move into deeper realms to fulfill their carbon demands. Our results show the importance of the under-ice fauna, particularly in controlling the carbon flux from the sea ice to deeper living communities.

Data accessibility statement

The datasets generated for this study are available on the PANGAEA database: https://doi.org/10.1594/PANGAEA.931610

https://doi.org/10.1594/PANGAEA.931140

Supplemental files

The supplemental files for this article can be found as follows:

Table S1. Carbon content, mass-specific ingestion rate, and trophic type for all taxa of sea-ice meiofauna (docx).

Table S2. Carbon content, mass specific ingestion rate, and trophic type for all taxa of under-ice fauna (docx).

Acknowledgments

We thank the Captain and crew of the *Polarstern* expedition PS92 for their support and guidance with work at sea. We thank Michiel van Dorssen and André Meijboom for their great help during the fieldwork. The Surface and Under-Ice Trawl for this study was kindly provided by Jan Andries van Franeker. We acknowledge support by the Open Access Publication Funds of Alfred-Wegener-Institut Helmholtz-Zentrum für Polar- und Meeresforschung.

Funding

JE was funded by the national scholarships "Promotionsstipendium nach dem Hamburger Nachwuchsfördergesetz (HmbNFG)" and "Gleichstellungsfond 2017 (4-GLF-2017)," both granted by the University of Hamburg. The German Academic Exchange Service (DAAD) and the graduate school "POLMAR" at Alfred Wegener Institute Bremerhaven supported JE's visit at The Arctic University of Norway's Institute of Arctic and Marine Biology. BAB's contribution was under the framework of the Arctic Seasonal Ice Zone Ecology project, cofunded by UiT The Arctic University of Norway and the Tromsø Research Foundation (Project Number 01vm/h15). IP, JE, GC, and HF were funded by the Polar Regions and Coasts in a Changing Earth System program of the Helmholtz Association and the expedition Grant No. AWI_PS92_00 and the program-oriented research Period 4 (POF4) Earth and Environment fund of the Helmholtz association. HF, JE, and GC were part of the Helmholtz Association Young Investigators Groups *Iceflux*: Ice-ecosystem carbon flux in polar oceans (VH-NG-800). GC is currently funded by the project *Eco-Light* (03V01465) as part of the joint NERC/BMBF program Changing Arctic Ocean. FLS received support from The Netherlands Ministry of Agriculture, Nature and Food Quality (LNV) under its Statutory Research Task Nature and Environment WOT-04-009-047.04. The Netherlands Polar Programme, managed by the Dutch Research Council (NWO), funded this research under project nr. ALW

866.13.009. AB work is funded by the Leibnitz Association.

Competing interests

The authors declare that the research was conducted in the absence of any commercial or financial relationships that could be construed as a potential conflict of interest.

Author contributions

JE, HF, AB, and BAB designed the study. HF, FLS, GC, and IP conducted the field work and sample collection. JE and BAB analyzed the meiofauna samples. JE and FLS analyzed the under-ice fauna samples. IP determined the chlorophyll *a* concentration in the sea-ice samples. GC modeled chl *a* concentration in the ice and the 0–2 water column for all Surface and Under-Ice Trawl stations. JE calculated the biomass of ice-algae and phytoplankton for all stations. PM calculated the primary production of ice algae and phytoplankton for all stations. JE calculated the biomass, carbon demand, and secondary production of sea-ice meiofauna and under-ice fauna for all stations. JE analyzed the data, wrote the article, and prepared all figures and tables. JE, BAB, HF, and IP contributed to data interpretation. All authors contributed to the article and approved its submission.

References

Ardyna, M, Arrigo, KR. 2020. Phytoplankton dynamics in a changing Arctic Ocean. *Nature Climate Change*. DOI: http://dx.doi.org/10.1038/s41558-020-0905-y.

Ardyna, M, Babin, M, Gosselin, M, Devred, E, Rainville, L, Tremblay, JÉ. 2014. Recent Arctic Ocean sea ice loss triggers novel fall phytoplankton blooms. *Geophysical Research Letters* **41**(17): 6207–6212.

Arndt, CE, Swadling, KM. 2006. Crustacea in Arctic and Antarctic sea ice: Distribution, diet and life history strategies. *Advances in Marine Biology* **51**:197–315. DOI: http://dx.doi.org/10.1016/s0065-2881(06)51004-1.

Arrigo, KR, van Dijken, GL. 2015. Continued increases in Arctic Ocean primary production. *Progress in Oceanography* **136**: 60–70.

Assmy, P, Fernández-Méndez, M, Duarte, P, Meyer, A, Randelhoff, A, Mundy, CJ, Olsen, LM, Kauko, HM, Bailey, A, Chierici, M. 2017. Leads in Arctic pack ice enable early phytoplankton blooms below snow-covered sea ice. *Scientific Reports* **7**: 40850.

Auel, H, Hagen, W. 2002. Mesozooplankton community structure, abundance and biomass in the central Arctic Ocean. *Marine Biology* **140**(5): 1013–1021.

Berge, J, Varpe, Ø, Moline, M, Wold, A, Renaud, P, Daase, M, Falk-Petersen, S. 2012. Retention of ice-associated amphipods: Possible consequences for an ice-free Arctic Ocean. *Biology Letters* **8**(6): 1012–1015.

Beszczynska-Möller, A, Fahrbach, E, Schauer, U, Hansen, E. 2012. Variability in Atlantic water temperature and transport at the entrance to the Arctic Ocean, 1997–2010. *ICES Journal of Marine Science* **69**(5): 852–863.

Bluhm, BA, Gebruk, AV, Gradinger, R, Hopcroft, RR, Huettmann, F, Kosobokova, KN, Sirenko, BI, Weslawski, JM. 2011. Arctic marine biodiversity an update of species richness and examples of biodiversity change. *Oceanography* **24**(3): 232–248.

Bluhm, BA, Hop, H, Vihtakari, M, Gradinger, R, Iken, K, Melnikov, IA, Soreide, JE. 2018. Sea ice meiofauna distribution on local to Pan-Arctic scales. *Ecology and Evolution* **8**(4): 2350–2364. DOI: http://dx.doi.org/10.1002/ece3.3797.

Bonnet, D, Richardson, A, Harris, R, Hirst, A, Beaugrand, G, Edwards, M, Ceballos, S, Diekman, R, López-Urrutia, A, Valdes, L. 2005. An overview of *Calanus helgolandicus* ecology in European waters. *Progress in Oceanography* **65**(1): 1–53.

Bradstreet, MS, Cross, WE. 1982. Trophic relationships at high Arctic ice edges. *Arctic* **35** (1): 1–12.

CAFF. 2017. *State of the Arctic Marine Biodiversity Report*. Akureyri, Iceland: Conservation of Arctic Flora and Fauna.

Campbell, RG, Ashjian, CJ, Sherr, EB, Sherr, BF, Lomas, MW, Ross, C, Alatalo, P, Gelfman, C, Van Keuren, D. 2016. Mesozooplankton grazing during spring sea-ice conditions in the eastern Bering Sea. *Deep Sea Research Part II: Topical Studies in Oceanography* **134**: 157–172.

Campitelli, E. 2019. ggnewscale: Multiple Fill and Color Scales in "ggplot2." R Package Version 0.2.0. Available at https://CRAN.R-project.org/package=ggnewscale. Accessed 1 October 2020.

Castellani, G, Losch, M, Lange, BA, Flores, H. 2017. Modeling Arctic sea-ice algae: Physical drivers of spatial distribution and algae phenology. *Journal of Geophysical Research: Oceans* **122**(9): 7466–7487.

Castellani, G, Schaafsma, FL, Arndt, S, Lange, BA, Peeken, I, Ehrlich, J, David, C, Ricker, R, Krumpen, T, Hendricks, S. 2020. Large-scale variability of physical and biological sea-ice properties in polar oceans. *Frontiers in Marine Science* **7**: 536.

Daase, M, Hop, H, Falk-Petersen, S. 2016. Small-scale diel vertical migration of zooplankton in the High Arctic. *Polar Biology* **39**(7): 1213–1223.

Dalpadado, P. 2002. Inter-specific variations in distribution, abundance and possible life-cycle patterns of *Themisto* spp. (Amphipoda) in the Barents Sea. *Polar Biology* **25**(9): 656–666.

Darnis, G, Barber, DG, Fortier, L. 2008. Sea ice and the onshore–offshore gradient in pre-winter zooplankton assemblages in southeastern Beaufort Sea. *Journal of Marine Systems* **74**(3–4): 994–1011.

Darnis, G, Hobbs, L, Geoffroy, M, Grenvald, JC, Renaud, P, Berge, J, Cottier, F, Kristiansen, S, Daase, M, Søreide, JE. 2017. From polar night to midnight sun: Diel vertical migration, metabolism and biogeochemical role of zooplankton in a high Arctic fjord (Kongsfjorden, Svalbard). *Limnology and Oceanography* **62**(4): 1586–1605.

Daufresne, M, Lengfellner, K, Sommer, U. 2009. Global warming benefits the small in aquatic ecosystems. *Proceedings of the National Academy of Sciences* **106**(31): 12788–12793.

David, C, Lange, B, Krumpen, T, Schaafsma, F, van Franeker, JA, Flores, H. 2016. Under-ice distribution of polar cod *Boreogadus saida* in the central Arctic Ocean and their association with sea-ice habitat properties. *Polar Biology* **39**(6): 981–994.

David, C, Lange, B, Rabe, B, Flores, H. 2015. Community structure of under-ice fauna in the Eurasian central Arctic Ocean in relation to environmental properties of sea-ice habitats. *Marine Ecology Progress Series* **522**: 15–32. DOI: http://dx.doi.org/10.3354/meps11156.

Deibel, D. 1988. Filter feeding by *Oikopleura vanhoeffeni*: Grazing impact on suspended particles in cold ocean waters. *Marine Biology* **99**(2): 177–186.

Dunnington, D. 2018. ggspatial: Spatial Data Framework for ggplot2. Available at https://CRAN.R-project.org/package=ggspatial. Accessed 1 October 2020.

Dupont, F. 2012. Impact of sea-ice biology on overall primary production in a biophysical model of the pan-Arctic Ocean. *Journal of Geophysical Research: Oceans* **117**(C8). DOI: http://dx.doi.org/10.1029/2011jc006983.

Ehrlich, J, Schaafsma, FL, Bluhm, BA, Peeken, I, Castellani, G, Brandt, A, Flores, H. 2020. Sympagic fauna in and under Arctic pack ice in the annual sea-ice system of the New Arctic. *Frontiers in Marine Science* **7**(452). DOI: http://dx.doi.org/10.3389/fmars.2020.00452.

Fernández-Méndez, M, Katlein, C, Rabe, B, Nicolaus, M, Peeken, I, Bakker, K, Flores, H, Boetius, A. 2015. Photosynthetic production in the central Arctic Ocean during the record sea-ice minimum in 2012. *Biogeosciences* **12**(11): 3525–3549.

Flores, H. 2009. Frozen desert alive. The role of sea ice for pelagic macrofauna and its predators: Implications for the Antarctic pack-ice food web. Available at http://epic.awi.de/30609/1/Flores_Frozen DesertAlive_std.pdf. Accessed 30 August 2020.

Flores, H, David, C, Ehrlich, J, Hardge, K, Kohlbach, D, Lange, BA, Niehoff, B, Nöthig, E-M, Peeken, I, Metfies, K. 2019. Sea-ice properties and nutrient concentration as drivers of the taxonomic and trophic structure of high-Arctic protist and metazoan communities. *Polar Biology* **42**(7): 1377–1395.

Forest, A, Coupel, P, Else, B, Nahavandian, S, Lansard, B, Raimbault, P, Papakyriakou, T, Gratton, Y, Fortier, L, Tremblay, J-É. 2014. Synoptic evaluation of carbon cycling in the Beaufort Sea during summer: Contrasting river inputs, ecosystem metabolism and air–sea CO_2 fluxes. *Biogeosciences* **11**(10): 2827–2856.

Fortier, M, Fortier, L, Hattori, H, Saito, H, Legendre, L. 2001. Visual predators and the diel vertical migration of copepods under Arctic sea ice during the midnight sun. *Journal of Plankton Research* **23**(11): 1263–1278.

Friedrich, C. 1997. Ökologische Untersuchungen zur Fauna des arktischen Meereises [Ecological investigations on the fauna of the Arctic sea-ice], Berichte zur Polarforschung [Reports on Polar Research], Bremerhaven, Alfred Wegener Institute for Polar and Marine Research, 246, 211 p. DOI: http://dx.doi.org/10.2312/BzP_0246_1997.

Garrison, DL, Buck, KR. 1986. Organism losses during ice melting: A serious bias in sea ice community studies. *Polar Biology* **6**(4): 237–239.

Gosselin, M, Levasseur, M, Wheeler, PA, Horner, RA, Booth, BC. 1997. New measurements of phytoplankton and ice algal production in the Arctic Ocean. *Deep Sea Research Part II: Topical Studies in Oceanography* **44**(8): 1623–1644.

Gradinger, R. 1999a. Integrated abundance and biomass of sympagic meiofauna in Arctic and Antarctic pack ice. *Polar Biology* **22**(3): 169–177.

Gradinger, R. 1999b. Vertical fine structure of the biomass and composition of algal communities in Arctic pack ice. *Marine Biology* **133**(4): 745–754.

Gradinger, R. 2009. Sea-ice algae: Major contributors to primary production and algal biomass in the Chukchi and Beaufort Seas during May/June 2002. *Deep Sea Research Part II: Topical Studies in Oceanography* **56**(17): 1201–1212.

Gradinger, R, Bluhm, BA. 2020. First analysis of an Arctic sea ice meiofauna food web based on abundance, biomass and stable isotope ratios. *Marine Ecology Progress Series* **634**: 29–43.

Gradinger, R, Friedrich, C, Spindler, M. 1999. Abundance, biomass and composition of the sea ice biota of the Greenland Sea pack ice. *Deep Sea Research Part II: Topical Studies in Oceanography* **46**(6–7): 1457–1472.

Gradinger, RR, Kaufman, MR, Bluhm, BA. 2009. Pivotal role of sea ice sediments in the seasonal development of near-shore Arctic fast ice biota. *Marine Ecology Progress Series* **394**: 49–63.

Grainger, E, Hsiao, SI. 1990. Trophic relationships of the sea ice meiofauna in Frobisher Bay, Arctic Canada. *Polar Biology* **10**(4): 283–292.

Granskog, MA, Fer, I, Rinke, A, Steen, H. 2018. Atmosphere-ice-ocean-ecosystem processes in a thinner Arctic sea ice regime: The Norwegian Young Sea ICE (N-ICE2015) expedition. *Journal of Geophysical Research: Oceans* **123**(3): 1586–1594.

Grebmeier, JM, Moore, SE, Overland, JE, Frey, KE, Gradinger, R. 2010. Biological response to recent Pacific Arctic sea ice retreats. *Eos, Transactions American Geophysical Union* **91**(18): 161–162.

Hop, H, Pavlova, O. 2008. Distribution and biomass transport of ice amphipods in drifting sea ice around Svalbard. *Deep Sea Research Part II: Topical Studies in Oceanography* **55**(20–21): 2292–2307.

Hop, H, Vihtakari, M, Bluhm, BA, Assmy, P, Poulin, M, Gradinger, R, Peeken, I, von Quillfeldt, C, Olsen, LM, Zhitina, L, Melnikov, IA. 2020. Changes in sea-ice protist diversity with declining sea ice in the Arctic Ocean from the 1980s to 2010s. *Frontiers in*

Marine Science **7**(243). DOI: http://dx.doi.org/10.3389/fmars.2020.00243.

Horner, R, Ackley, SF, Dieckmann, GS, Gulliksen, B, Hoshiai, T, Legendre, L, Melnikov, IA, Reeburgh, WS, Spindler, M, Sullivan, CW. 1992. Ecology of sea ice biota. *Polar Biology* **12**(3–4): 417–427.

Kassambara, A. 2020. ggpubr: 'ggplot2' Based Publication ReadyPlots. R Package Version 0.4.0. Available at https://CRAN.R-project.org/package=ggpubr. Accessed 1 October 2020.

Kiko, R, Kern, S, Kramer, M, Mütze, H. 2017. Colonization of newly forming Arctic sea ice by meiofauna: A case study for the future Arctic?*Polar Biology* **40**(6): 1277–1288.

Kohlbach, D, Graeve, MA, Lange, B, David, C, Peeken, I, Flores, H. 2016. The importance of ice algae-produced carbon in the central Arctic Ocean ecosystem: Food web relationships revealed by lipid and stable isotope analyses. *Limnology and Oceanography* **61**(6): 2027–2044.

Kohlbach, D, Schaafsma, FL, Graeve, M, Lebreton, B, Lange, BA, David, C, Vortkamp, M, Flores, H. 2017. Strong linkage of polar cod (*Boreogadus saida*) to sea ice algae-produced carbon: Evidence from stomach content, fatty acid and stable isotope analyses. *Progress in Oceanography* **152**: 62–74.

Kosobokova, K, Hirche, H-J. 2009. Biomass of zooplankton in the eastern Arctic Ocean—A base line study. *Progress in Oceanography* **82**(4): 265–280.

Kramer, M. 2011. The role of sympagic meiofauna in Arctic and Antarctic sea-ice food webs [dissertation]. Kiel, Germany: Christian-Albrechts Universität zu Kiel.

Krumpen, T, Belter, HJ, Boetius, A, Damm, E, Haas, C, Hendricks, S, Nicolaus, M, Nöthig, E-M, Paul S, Peeken, I. 2019. Arctic warming interrupts the Transpolar Drift and affects long-range transport of sea ice and ice-rafted matter. *Scientific Reports* **9**(1): 5459.

Lange, BA, Katlein, C, Castellani, G, Fernández-Méndez, M, Nicolaus, M, Peeken, I, Flores, H. 2017. Characterizing spatial variability of ice algal chlorophyll a and net primary production between sea ice habitats using horizontal profiling platforms. *Frontiers in Marine Science* **4**: 349.

Lange, BA, Katlein, C, Nicolaus, M, Peeken, I, Flores, H. 2016. Sea ice algae chlorophyll a concentrations derived from under-ice spectral radiation profiling platforms. *Journal of Geophysical Research: Oceans* **121**(12): 8511–8534.

Leu, E, Mundy, C, Assmy, P, Campbell, K, Gabrielsen, T, Gosselin, M, Juul-Pedersen, T, Gradinger, R. 2015. Arctic spring awakening–Steering principles behind the phenology of vernal ice algal blooms. *Progress in Oceanography* **139**: 151–170.

Leu, E, Søreide, J, Hessen, D, Falk-Petersen, S, Berge, J. 2011. Consequences of changing sea-ice cover for primary and secondary producers in the European Arctic shelf seas: Timing, quantity, and quality. *Progress in Oceanography* **90**(1–4): 18–32.

Lewis, MR, Smith, JC. 1983. A small volume, short-incubation-time method for measurement of photosynthesis as a function of incident irradiance. *Marine Ecology Progress Series* **13**(1): 99–102.

Li, WK, McLaughlin, FA, Lovejoy, C, Carmack, EC. 2009. Smallest algae thrive as the Arctic Ocean freshens. *Science* **326**(5952): 539–539.

Lindeman, RL. 1942. The trophic-dynamic aspect of ecology. *Ecology* **23**(4): 399–417.

Lønne, O, Gulliksen, B. 1991. Sympagic macro-fauna from multiyear sea-ice near Svalbard. *Polar Biology* **11**(7): 471–477.

Marquardt, M, Kramer, M, Carnat, G, Werner, I. 2011. Vertical distribution of sympagic meiofauna in sea ice in the Canadian Beaufort Sea. *Polar Biology* **34**(12): 1887–1900. DOI: http://dx.doi.org/10.1007/s00300-011-1078-y.

Massicotte, P, Peeken, I, Katlein, C, Flores, H, Huot, Y, Castellani, G, Arndt, S, Lange, BA, Tremblay, JÉ, Babin, M. 2019. Sensitivity of phytoplankton primary production estimates to available irradiance under heterogeneous sea ice conditions. *Journal of Geophysical Research: Oceans* **124**(8): 5436–5450.

Matrai, P, Olson, E, Suttles, S, Hill, V, Codispoti, L, Light, B, Steele, M. 2013. Synthesis of primary production in the Arctic Ocean: I. Surface waters, 1954–2007. *Progress in Oceanography* **110**: 93–106.

Moloney, CL, Field, JG. 1989. General allometric equations for rates of nutrient uptake, ingestion, and respiration in plankton organisms. *Limnology and Oceanography* **34**(7): 1290–1299.

Moran, S, Kelly, R, Hagstrom, K, Smith, J, Grebmeier, J, Cooper, L, Cota, G, Walsh, J, Bates, N, Hansell, DA. 2005. Seasonal changes in POC export flux in the Chukchi Sea and implications for water column-benthic coupling in Arctic shelves. *Deep Sea Research Part II: Topical Studies in Oceanography* **52**(24–26): 3427–3451.

Nicolaus, M, Katlein, C. 2013. Mapping radiation transfer through sea ice using a remotely operated vehicle (ROV). *The Cryosphere* **7**: 763–777.

Nöthig, E-M, Lalande, C, Fahl, K, Metfies, K, Salter, I, Bauerfeind, E. 2020. Annual cycle of downward particle fluxes on each side of the Gakkel Ridge in the central Arctic Ocean. *Philosophical Transactions of the Royal Society A* **378**(2181): 20190368.

Nozais, C, Gosselin, M, Michel, C, Tita, G. 2001. Abundance, biomass, composition and grazing impact of the sea-ice meiofauna in the North Water, northern Baffin Bay. *Marine Ecology Progress Series* **217**: 235–250. DOI: http://dx.doi.org/10.3354/meps217235.

Pante, E, Simon-Bouhet, B. 2013. marmap: A package for importing, plotting and analyzing bathymetric and topographic data in R. *PLoS One* **8**(9): e73051.

Pebesma, EJ. 2018. Simple features for R: Standardized support for spatial vector data. *R J* **10**(1): 439.

Peeken, I. 2020. Chemtax Based Phytoplankton Group Composition During POLARSTERN Cruise PS92 [dataset]. DOI: http://dx.doi.org/10.1594/PANGAEA.917802.

Polyakov, IV, Pnyushkov, AV, Alkire, MB, Ashik, IM, Baumann, TM, Carmack, EC, Goszczko, I, Guthrie, J, Ivanov, VV, Kanzow, T, Krishfield, R, Kwok, R, Sundfjord, A, Morison, J, Rembe,r R, Yulin, A. 2017. Greater role for Atlantic inflows on sea-ice loss in the Eurasian Basin of the Arctic Ocean. *Science* **356**(6335): 285–291. DOI: http://dx.doi.org/10.1126/science.aai8204.

Poulin, M, Daugbjerg, N, Gradinger, R, Ilyash, L, Ratkova, T, von Quillfeldt, C. 2011. The pan-Arctic biodiversity of marine pelagic and sea-ice unicellular eukaryotes: A first-attempt assessment. *Marine Biodiversity* **41**(1): 13–28.

Raskoff, K, Hopcroft, R, Kosobokova, K, Purcell, J, Youngbluth, M. 2010. Jellies under ice: ROV observations from the Arctic 2005 hidden ocean expedition. *Deep Sea Research Part II: Topical Studies in Oceanography* **57**(1–2): 111–126.

Richardson, AJ. 2008. In hot water: Zooplankton and climate change. *ICES Journal of Marine Science* **65**(3): 279–295.

Rudels, B, Schauer, U, Björk, G, Korhonen, M, Pisarev, S, Rabe, B, Wisotzki, A. 2013. Observations of water masses and circulation in the Eurasian Basin of the Arctic Ocean from the 1990s to the late 2000s. *OS Special Issue: Ice-Atmosphere-Ocean interactions in the Arctic Ocean during IPY: The Damocles Project* **9**(1): 147–169.

Saito, H, Kiørboe, T. 2001. Feeding rates in the chaetognath *Sagitta elegans*: Effects of prey size, prey swimming behaviour and small-scale turbulence. *Journal of Plankton Research* **23**(12): 1385–1398.

Scott, CL, Falk-Petersen, S, Sargent, JR, Hop, H, Lønne, OJ, Poltermann, M. 1999. Lipids and trophic interactions of ice fauna and pelagic zooplankton in the marginal ice zone of the Barents Sea. *Polar Biology* **21**(2): 65–70.

Søreide, JE, Carroll, ML, Hop, H, Ambrose, WG Jr., Hegseth, EN, Falk-Petersen, S. 2013. Sympagic-pelagic-benthic coupling in Arctic and Atlantic waters around Svalbard revealed by stable isotopic and fatty acid tracers. *Marine Biology Research* **9**(9): 831–850.

Søreide, JE, Leu, E, Berge, J, Graeve, M, Falk-Petersen, S. 2010. Timing of blooms, algal food quality and *Calanus glacialis* reproduction and growth in a changing Arctic. *Global Change Biology* **16**(11): 3154–3163.

South, A. 2017. rnaturalearth: World map data from natural earth. R Package Version 0.1.0. Available at https://CRAN.R-project.org/package=rnaturalearth. Accessed 1 September 2020.

South, A. 2020. rnaturalearthhires: High resolution world vector map data from natural earth used in rnaturalearth. R Package Version 0.1.0. Available at https://github.com/ropensci/rnaturalearthhires. Accessed 1 September 2020.

Stevens, C, Deibel, D, Parrish, C. 2004. Species-specific differences in lipid composition and omnivory indices in Arctic copepods collected in deep water during autumn (North Water Polynya). *Marine Biology* **144**(5): 905–915.

R Core Team. 2018. R: A language and environment for statistical computing: A graduate course in probability. Vienna, Austria: R Foundation for Statistical Computing.

Tedesco, L, Vichi, M, Scoccimarro, E. 2019. Sea-ice algal phenology in a warmer Arctic. *Science Advances* **5**(5): eaav4830.

Tran, S, Bonsang, B, Gros, V, Peeken, I, Sarda-Esteve, R, Bernhardt, A, Belvisio, S. 2013. A survey of carbon monoxide and non-methane hydrocarbons in the Arctic Ocean during summer 2010. *Biogeosciences* **10**: 1909–1935.

Verity, PG. 1991. Measurement and simulation of prey uptake by marine planktonic ciliates fed plastidic and aplastidic nanoplankton. *Limnology and Oceanography* **36**(4): 729–750.

Verity, PG, Wassmann, P, Frischer, M, Howard-Jones, M, Allen, A. 2002. Grazing of phytoplankton by microzooplankton in the Barents Sea during early summer. *Journal of Marine Systems* **38**(1–2): 109–123.

Vernet, M, Richardson, TL, Metfies, K, Nöthig, E-M, Peeken, I. 2017. Models of plankton community changes during a warm water anomaly in arctic waters show altered trophic pathways with minimal changes in carbon export. *Frontiers in Marine Science* **4**: 160.

Welch, HE, Bergmann, MA, Siferd, TD, Martin, KA, Curtis, MF, Crawford, RE, Conover, RJ, Hop, H. 1992. Energy flow through the marine ecosystem of the Lancaster Sound region, Arctic Canada. *Arctic* **45**(4): 343–357.

Werner, I. 1997. Grazing of Arctic under-ice amphipods on sea-ice algae. *Marine Ecology Progress Series* **160**: 93–99.

Werner, I. 2006. Seasonal dynamics of sub-ice fauna below pack ice in the Arctic (Fram Strait). *Deep Sea Research Part I: Oceanographic Research Papers* **53**(2): 294–309.

Werner, I, Auel, H. 2005. Seasonal variability in abundance, respiration and lipid composition of Arctic under-ice amphipods. *Marine Ecology Progress Series* **292**: 251–262.

Wickham, H. 2016. *ggplot2: Elegant graphics for data analysis*. New York, NY: Springer-Verlag.

Wickham, H. 2018. Scales: Scale functions for visualization. R Package Version 1.0.0. Available at https://CRAN.R-project./package=scales. Accessed 1 August 2020.

Wiedmann, I, Ershova, E, Bluhm, BA, Nöthig, E-M, Gradinger, RR, Kosobokova, K, Boetius, A. 2020. What feeds the benthos in the Arctic Basins? Assembling a carbon budget for the deep Arctic Ocean. *Frontiers in Marine Science* **7**: 224.

How to cite this article: Ehrlich, J, Bluhm, BA, Peeken, I, Massicotte, P, Schaafsma, FL, Castellani, G, Brandt, A, Flores, H. 2021. Sea-ice associated carbon flux in Arctic spring. *Elementa: Science of the Anthropocene* 9(1). DOI: https://doi.org/10.1525/elementa.2020.00169

Domain Editor-in-Chief: Jody W. Deming, University of Washington, Seattle, WA, USA

Associate Editor: Jean-Éric Tremblay, Department of Biology, Université Laval, Québec City, Québec, Canada

Knowledge Domain: Ocean Science

Part of an Elementa Special Feature: Insights into Biogeochemical Exchange Processes at Sea Ice Interfaces (BEPSII-2)

Published: October 13, 2021 **Accepted:** September 4, 2021 **Submitted:** November 16, 2020

ELEMENTA Science of the Anthropocene

Elem Sci Anth is a peer-reviewed open access journal published by University of California Press.

OPEN ACCESS